Synthesis of Transition Metal Boride Nanoparticles by Induction Thermal Plasma

L. Liu, Y. Tanoue, T. Nonaka, M. Tanaka and T. Watanabe

Department of Chemical Engineering, Faculty of Engineering, Kyushu University, 744 Motooka, Nishi-ku, Fukuoka 819-0395, Japan

Abstract: Tungsten boride and molybdenum boride nanoparticles were successfully synthesized by induction thermal plasma. The different composition of metal (W or Mo) to boron was changed to investigate the formation mechanism of metal boride nanoparticles. The calculated nucleation temperature clarified that the reactions of Mo-B system can occur more easily than that of W-B system. The products of W-B system showed greater deviation from the thermodynamic equilibrium phase than Mo-B system.

Keywords: Thermal plasma, metal boride nanoparticles, nucleation temperature.

1. Introduction

The induction thermal plasma synthesis of nanoparticles is a promising method because of its unique fluid dynamics, thermodynamic and chemical features [1, 2], such as high enthalpy which enhances reaction kinetics (even up to 10^4 K), high chemical reactivity, large plasma volume and high cooling rate (10^4–10^6 K/s). Furthermore, the thermal plasma can be generated in a plasma torch without internal electrodes [3, 4], which if combined with its wide range of operating parameters, induction thermal plasma can be considered as an innovative and powerful tool for synthesis of functional nanoparticles with high purity.

Transition metal boride (TMB) is an important class of advanced structural materials. Its special properties of high melting points, hardness, high thermal and electric conductivity, great thermal stability and especially considerable resistance to oxidation in air make TMB viable candidate materials for various applications. Tungsten and molybdenum borides are known for industrial applications as abrasive, corrosion-resistant and electrode materials which are exposed at elevated temperatures and in corrosive media.

Induction thermal plasma can perform outstandingly when synthesizing tungsten and molybdenum boride nanoparticles with high-purity, irrespective of the high melting points of boron and metals [5]. This study is aim to synthesize TMB nanoparticles produced by changing the feeding composition ratio of different metals to boron and to understand its formation mechanism.

2. Experiment

2.1 Experimental Setup and Conditions

The synthesis apparatus, includes a plasma torch, a reaction chamber, and a recovery unit, which are presented in **Fig. 1**. The induction thermal plasma torch consists of a coil surrounding water-cooled refractory tube. The raw materials are supplied as powders along with the carrier gas and injected into the plasma torch. Then, they evaporate instantly and nanoparticles are produced through homogeneous nucleation in the high temperature region and subsequent heterogeneous condensation in the tail region of plasma flame. The formed nanoparticles are collected on the wall of the filter.

Table 1 shows the experimental conditions for nanoparticle synthesis under atmospheric pressure. Argon was used as the carrier and inner gases. The reaction chamber was placed below the torch. The raw materials are composed of B (45 μm, 99.9%, Kojundo Chemical

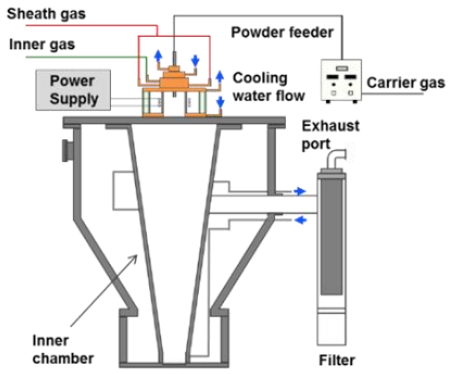

Fig. 1. Experimental configuration of RF thermal plasma for nanoparticle synthesis.

Table 1. Experimental conditions of the RF thermal plasma system.

Input power [kW]	20
RF frequency [MHz]	4
Pressure [kPa]	101.3
Sheath gas rate [L/min]	60 (Ar)
Inner gas rate [L/min]	5 (Ar)
Carrier gas rate [L/min]	3 (Ar)
Discharge time [min]	6
Mean diameter [μm]	45
Feed rate [g/min]	0.3
Powder mole fraction	(W or Mo):B=1:0.5, 1:1, 1:2, 1:2.5, 1:4, 1:6

Laboratory) and metals including W (0.6 μm, 99.9%, Kojundo Chemical Laboratory) and Mo (1.5 μm, 99.9%, Kojundo Chemical Laboratory). Metal and B particles were mixed at a given composition before they were introduced into the plasma at a feed rate of 0.3 g/min, where the composition of both W-B system and Mo-B system is summarized in Table 1. The total system was evacuated and then argon was introduced until the pressure was raised to atmospheric pressure. A small amount of oxygen was injected after experiment to prevent the further oxidation of synthesized nanoparticles to form a larger diameter.

2.2 Analysis

The phase composition of products and mass fraction of metal boride was measured by X-ray diffractometry (XRD, Rigaku Multiflex), operating with a Cu Kα source (λ = 0.1541 nm). The particle's morphology was observed by transmission electron microscopy (TEM, JEOL JEM-2100HCKM) at 200 kV for electron accelerating voltage, and size distributions were measured by counting approximately 200 different particles. Element mapping of nanoparticles was analysed by scanning TEM-energy dispersive X-ray spectrometry (STEM-EDS, JEOL JEM-ARM 200F).

3. Results and discussion

The XRD patterns of nanoparticles synthesized at different ratios of metal to boron, (W or Mo):B, in feeding powders are presented in **Figs. 2** and **3**, respectively. The nanoparticles are identified as metal boride and unreacted metal. Metal borides can be synthesized and increased with B content in feeding materials. Tungsten boride appeared at the condition of W:B=1:2; and molybdenum boride appeared at lower B content condition of Mo:B=1:1. The intensity of unreacted W is high even on the condition of W:B=1:4, while Mo significantly decreased on a lower B content condition of Mo:B=1:2.5. Apparently, the reaction of Mo-B system is easier to occur than W-B system.

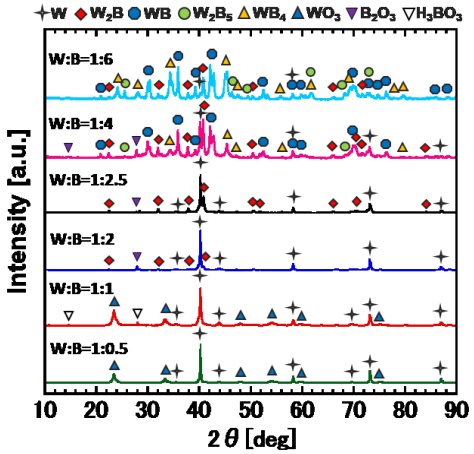

Fig. 2. XRD spectra of nanoparticles for W-B system with different composition ratios: W:B=1:6, 1:4, 1:2.5,1:2, 1:1 and 1:0.5.

Significant amount of B was oxidized and distinguished by XRD as B_2O_3 and H_3BO_3. B_2O_3 was anticipated as a by-product when synthesized B was partially oxidized after the experiment. B_2O_3 tends to react with water vapour in air and become H_3BO_3.

The relative integrated intensity of prepared particles was calculated according to the XRD results as shown in

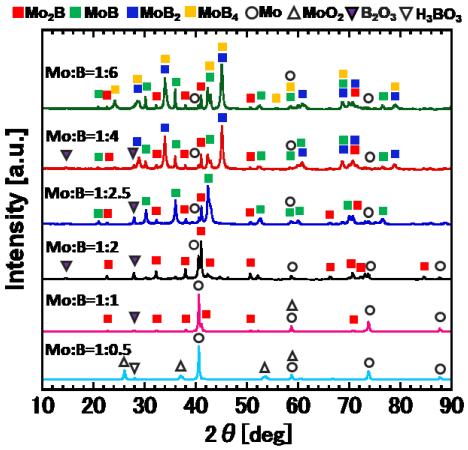

Fig. 3. XRD spectra of nanoparticles for Mo-B system with different composition ratios: Mo:B=1:6, 1:4, 1:2.5,1:2, 1:1 and 1:0.5.

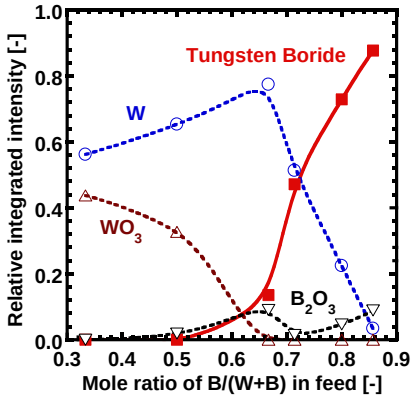

Fig. 4. Relative integrated intensity of nanoparticles with different B/(W+B) in W-B system.

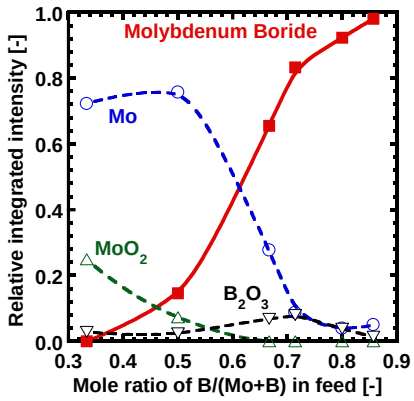

Fig. 5. Relative integrated intensity of nanoparticles with different B/(Mo+B) in Mo-B system.

Fig. 4 for W-B system and **Fig. 5** for Mo-B system. Relative integrated intensity is defined as the ratio of the integrated intensity of the highest peak from each product to the sum of the highest peaks from all products. The synthesized tungsten boride and molybdenum boride increased with the B content in raw materials. On the condition of (W or Mo):B=1:6, the highest content of metal borides of products was observed. The content of metal boride reached 87.7% in W-B system and 98.1% in Mo-B system separately. Under the same condition, Mo and B react more efficiently than with W and B.

Representative TEM images for different metal to boron ratio of raw materials are shown in **Fig. 6**. Spherical shaped particles are typically produced in all conditions. Polyhedron shape and rod-like particles were recognized in Mo rich condition, while hexagonal shape and some polyhedron shape of particles usually appeared in W rich condition. Mean diameter of nanoparticles were (a)14 nm and (b) 16 nm.

Element mapping images by STEM-EDS for synthesized nanoparticles on condition of W:B=1:4 and Mo:B=1:4 are presented in **Figs. 7** and **8**, respectively. These results showed that the mappings of metal and B overlapped in all particles. In other words, metal boride nanoparticles were successfully formed in both systems.

Homogeneous nucleation temperatures of metals considered in the present study were estimated based on nucleation theory considering non-dimensional surface tension [6]. The homogeneous nucleation rate J can be expressed as:

$$J = \frac{\beta_{ij} {n_s}^2 S}{12} \sqrt{\frac{\Theta}{2\pi}} \exp\left[\Theta - \frac{4\Theta^3}{27(\ln S)^2}\right] \quad (1)$$

where S is the saturation ratio and n_s is the equilibrium saturation monomer concentration at temperature T. β is the collision frequency function. The dimensionless surface tension is given by the following equation:

$$\Theta = \frac{\sigma s_1}{kT} \quad (2)$$

where σ is the surface tension and s_1 is the monomer surface area. The surface tension and the saturation ratio have a dominant influence on determining the nucleation rate.

The relationship between the calculated nucleation temperature and the melting point is summarized in **Fig. 9**. In low B content condition, Mo nucleates first and then the vapors of B condense onto the Mo nuclei to form molybdenum boride, while in high B content condition, B nucleates first and then the vapors of Mo condense onto the B nuclei. In contrast, W nucleates first in any condition with different B content, then the vapors of B condense onto the W nuclei to form tungsten boride. The nucleation temperature of B increases with the B content of raw materials, lead to a larger temperature range between B nucleation temperature and B melting point. Therefore, the co-condensation process lasts longer time due to the larger temperature range where the B vapors and metal vapors can mix well, result in the better synthesis of metal boride nanoparticles. This suggests that the condition of (W or

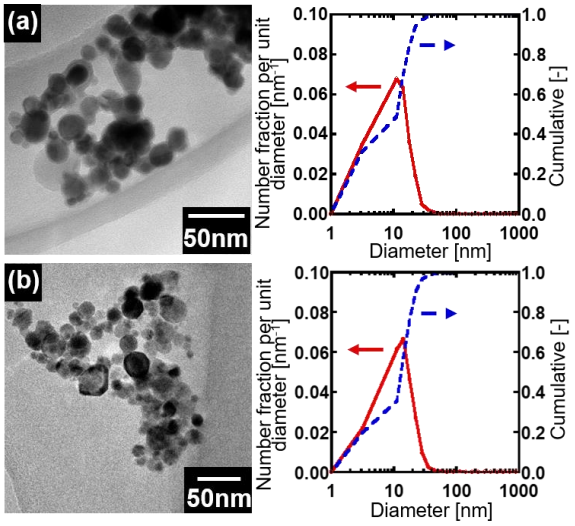

Fig. 6. Representative TEM images and mean size distribution of nanoparticles prepared under B rich condition: (a) W:B=1:4; (b) Mo:B=1:4.

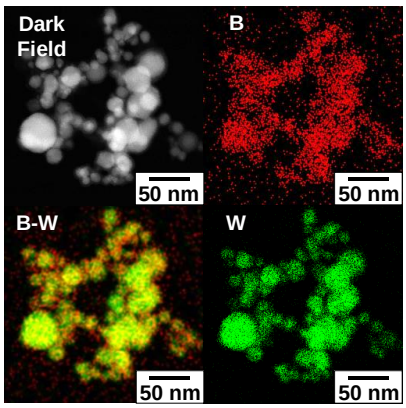

Fig. 7. Electron mapping of synthesized nanoparticles at W:B=1:4.

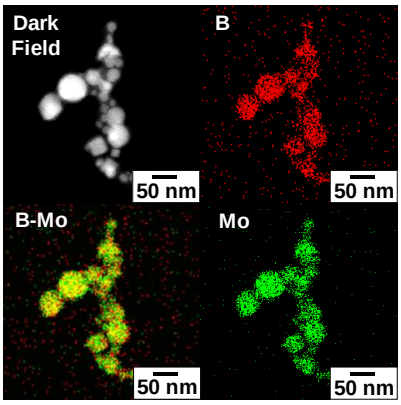

Fig. 8. Electron mapping of synthesized nanoparticles at Mo:B=1:4.

Mo):B=1:6 is the best condition to synthesize metal boride. This conclusion also agrees with the XRD analysis results.

The comparison between synthesized products and expected products according to the thermodynamic equilibrium of each system [7, 8] are listed in **Table 2**. Induction thermal plasma demonstrated a unique way to synthesize TMB, which did not strictly conform to the thermodynamics of phase diagram even though the mixed powders of precursors are supplied with the stoichiometric composition. At a certain composition, for example, some expected phases of WB and W_2B at composition of W:B=1:1 were skipped over due to the fast cooling temperature, while on B rich condition of W:B=1:6, some unexpected phases of WB and W_2B at lower B composition will be preserved due to the quenching effect. Furthermore, on the condition of (W or Mo):B=1:2, ratio of products W_2B and W were calculated as 15.0% and 85.0%, respectively, while Mo_2B and Mo were 78.3% and 21.7%, respectively. The products of W-B system showed greater deviation from the phase diagram than those of Mo-B system.

The deviation can be attributed to the nucleation temperature difference between metals and B which are mentioned above, as well as thermodynamic stability of each system. The negative Gibbs free energy of reaction of Mo_2B and W_2B indicated they can take place spontaneously. Following nucleation, supersaturated B vapors and metal vapors heterogeneous condense onto the nuclei, resulting in the formation of boride nanoparticles. For the condition of (W or Mo):B=1:2, the condensation of B vapors start at 2914 K, which is far below the nucleation temperature as well as the melting point of W in W-B system. This indicates the reaction between W and B becomes extremely difficult, because W has reached the melting point and started to solidify before B vapors start to condense. However, in Mo-B system, the condensation temperature of B is almost close to the nucleation temperature of Mo in Mo-B system. Mo and B are considered well-mixed in a liquid state in this co-condensation process since the particles grow at the temperature higher than the melting points of Mo and B, lead to better preparation of thermodynamically stable borides. These calculative agreements sufficiently support the present results and discussion.

4. Conclusion

Transition metal boride nanoparticles were successfully synthesized by induction thermal plasma. The content of tungsten boride and molybdenum boride nanoparticles in products increases with the boron content of raw materials. The formation mechanism was investigated on the basis of the homogenous nucleation temperature. Mo and B react more easily than W and B. The products of W-B system showed greater deviation from the phase diagram. Induction thermal plasma can provide a high efficient way to synthesize transition metal borides even though refractory metal borides to apply for large-scale industrial production.

Table 2. The synthesized products and expected products according to the phase diagram of each system.

	Molar ratio	main product	expected product
W-B system	1:0.5	W	W_2B, W
	1:1	W	WB, W_2B_5
	1:2	W, W_2B	WB, W_2B_5
	1:2.5	W, W_2B	W_2B_5, WB_4, B
	1:4	W_2B, WB, WB_4,W_2B_5, W	W_2B_5, WB_4, B
	1:6	WB, WB_4, W_2B,W_2B_5,W	W_2B_5, WB_4, B
Mo-B system	1:0.5	Mo	Mo_2B, Mo
	1:1	Mo, Mo_2B	MoB, Mo_2B, Mo
	1:2	Mo_2B, Mo	Mo_2B, MoB_2, MoB_4, B
	1:2.5	MoB, Mo_2B, Mo	MoB_2, Mo_2B_5, MoB_4, B
	1:4	MoB_2, MoB, Mo_2B, Mo	Mo_2B_5, MoB_4, B
	1:6	MoB_2, MoB_4, MoB, Mo_2B, Mo	Mo_2B_5, MoB_4, B

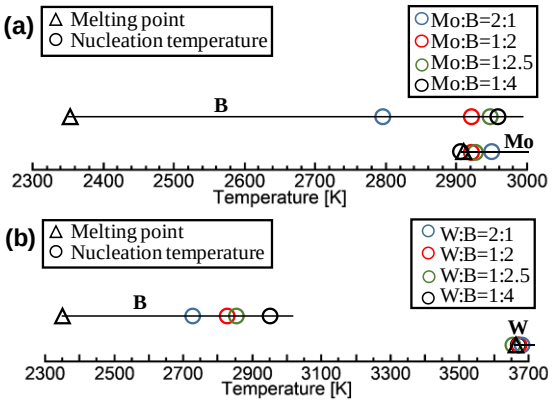

Fig. 9. Relationship between melting point and nucleation temperature of (a) Mo-B system and (b) W-B system.

5. References

[1] S.L. Girshick, et al., The Journal of Chemical Physics, **93**, 1273 (1989).

[2] M. Shigeta, et al., Journal of Physics D: Applied Physics, **44**, 174025 (2011).

[3] T. Watanabe, et al., Thin Solid Films **27**, 435 (2003).

[4] J. Szépvölgyi, et al., Plasma Chemistry and Plasma Processing, **26**, 597 (2006).

[5] Y. Cheng, et al., Chemical Engineering Journal, **183**, 483 (2012).

[6] S.L. Girshick, et al., Aerosol Science and Technology, **13**, 465 (1990).

[7] W.G. Moffatt. Handbook of Binary Phase Diagrams. Schenectady: Business Growth Services, General Electric Co., (1976).

[8] K.E. Spear, et al., Alloy Phase Diagram, 9, 4 (1988).